Experimental Mechanics (2012) 52:447–459
DOI 10.1007/s11340-011-9504-1

An Electromagnetic System for the Non-Contact Excitation of Bladed Disks

C.M. Firrone · T. Berruti

Received: 1 December 2010 / Accepted: 26 April 2011 / Published online: 12 May 2011

Abstract In this paper a non-contact excitation system based on electromagnets is described. The system aims at exciting cyclically symmetric structures like bladed disks by generating typical engine order-like travelling wave excitations that bladed disks encounter during service. Detailed description of the analytical formulation for the electromagnets sizing, quality assessment and practical implications of the final assembly for the bladed disk excitation are addressed. In particular, the paper proposes an original method to setup the excitation system in order to perform step-sine controlled force measurements. This feature is necessary when non-linear forced response must be measured on bladed disks in order to characterize the dynamic behaviour at different level of excitation. Typical applications of the designed excitation system are two: the first is the study of the effect of a force pattern characterized by a particular engine order on the forced response of mistuned bladed disks, the second is the characterization of intentional non-linear damping source occurring, for instance, for friction phenomena in presence of shrouds or underplatform dampers.

Keywords Noncontact excitation · Electromagnet · Bladed disks · Mistuning · Nonlinear · Dynamics

Introduction

Rotating components of turbo-machinery convert the energy of a fluid passing through the blade arrays of rotors into mechanical work (turbine) and vice versa (compressors). Basically, two main features of the bladed disk design concerning the dynamic response must be considered. On one hand the single rotor is subjected to an excitation pattern where each blade is loaded with a series of pulses within a complete disk rotation. The number and the intensity of pulses depend on the architecture of the engine preceding the rotor (number of combustion chambers, stages, stator vanes) and the wide spectral content is usually characterized by several harmonic components whose excitation frequencies on each blade are mainly a multiple of the rotor angular speed. The integer number which, multiplied by the rotor angular speed, gives the blade excitation frequency is known as engine order index (*eo*). On the other hand, a rotating disk is nominally characterized by cyclic symmetry properties where one fundamental sector constituted by the blade and its associated disk sector is repeated for a number of times around the rotation axis. The periodical repetition of geometric and material features (*tuned* system) generates a particular dynamic behaviour of the disk where natural frequencies, and corresponding modes, can be grouped into families featuring the same deformed shape of the vibrating blades or disk [1]. The dynamic study of the bladed disk through FE models benefits of this property since the modal analysis or the forced response calculation of the whole rotor can be performed by processing the mass and stiffness matrices of a single FE sector by applying cyclic symmetry boundary conditions at the interfaces shared with the contiguous sectors [2]. The bladed disk behaviour is obtained in post-processing by expanding the results of the fundamental sector to the real configuration.

The main objective at design stage is to avoid any match of the rotor natural frequencies with the excitation frequencies of the harmonic components of the load spectrum which thus shorten the life of the component

C.M. Firrone (✉) · T. Berruti
Department of Mechanical Engineering, Politecnico di Torino,
Corso Duca degli Abruzzi, 24,
Torino, Italy
e-mail: christian.firrone@polito.it

T. Berruti
e-mail: teresa.berruti@polito.it

due to the increased stress causing HCF failure. Unfortunately, bladed disk dynamics may show unexpected response due to small differences between sectors nominally identical which determine a *mistuned* configuration of the system [1, 3]. In worst cases, a distorted and localized forced response occurs in particular for high modal density regions where one or more blades vibration amplitude is higher than the tuned response. Causes of mistuning are manifold: irregularities associated to the material properties, asymmetry generated during assembly or during service due to wear assessment, different contact condition at the blade root joints, snubbers, shrouds in case of non-integral bladed disks, Foreign Object Damage (FOD) or modifications introduced during maintenance and repair processes. Another source of mistuning comes from the so-called underplatform dampers (UPDs) which are metal parts located within cavities between contiguous blades. UPDs' aim is to limit the vibration amplitude of blades in case of excitation at resonance by means of friction damping at the contact surfaces. Mistuning is introduced at the contacts which couple directly the blades subjected to wear and modifications in the contacts position during service. Interesting studies were carried out where UPDs are seen not only as a further source of mistuning to take into account but also as a mean to mitigate negative effects of inherent mistuning [4, 5] even by distributing a number of UPDs smaller than the number of the blades [6], or by systematically using UPDs having different mass [7].

Mistuning identification and validation of predicted results by application of intentional mistuning must be performed on dummy or real disks. Test campaigns are performed on test rigs which can be classified in two groups having a basic dual property: the first group has rotating disks with fixed excitation source, on the contrary the second group supports a static rotor excited by a travelling excitation. Both test rigs groups have advantages and limitations which must be addressed with respect to the objective of the test campaign. Rigs with rotating test articles are generally more complex than static rigs first of all due to the design of the disk containment which must fulfil safety requirements in case of blade release (usually they are built in a pit or within a protective bunker). Moreover, different levels of complexity are found in the comprehension of the mistuning phenomenon if tests are performed on real engines and cold flow rigs since fluid–structure interaction must be considered. In detail, correlations between mistuning and aero-coupling, damping and elastic effects of gas flow which decreases the magnification factor of the mistuned response [8], and the influence of mistuning on flutter instabilities onset can be studied. On the contrary, fluid-dynamics effects can be avoided by using a vacuum chamber (spin test rig). For both types of rotating rigs, however, gyroscopic and centrifugal force effects (e.g., blades untwisting, dependence of UPDs contact pressure on disk velocity) are taken into account. The excitation provided by the gas flow must be substituted in the vacuum rigs with an alternative source. Broad applications of non-contact excitation provided by magnetic fields are found in literature by means of permanent magnets or electromagnets whose attractive force is exerted on ferritic bladed disks.

The travelling wave excitation for static rigs is generated by contacting (piezo-actuators [9], shakers [10]) or non-contacting systems (electromagnets with AC feeding [11], speakers [12, 13]). Whatever the case, a control system must be purposely developed in order to activate the exciters with a given phase shift in time to mimic the engine order force pattern. Since the bladed disk does not rotate, the dynamic response is directly measured on the reference system fixed to the rotor by using non-contact devices like the scanning laser vibrometer [10, 14]. Since aerodynamic coupling effects are avoided as well as complications given by data transmission like in rotating disks, static test rigs allows to easily collect measurements of the dynamics of dummy or real bladed disks directly related to mistuning. The static test rigs are therefore suitable for validating mistuning identification methods and reduction techniques with precision.

When non-linear phenomena due to friction are present, the control of the force input is of primary importance since the forced response is strongly influenced by the amount of the local displacements of the structure at the contact surfaces. As a consequence attention must be paid to the measurement of the force pattern both for rotating and not rotating disks. Forces generated by air jets, for instance, can be measured with manometer probes which measure the pressure field before tests [15] or with probes embedded in the surface of the blades [5] or estimated as in [16] by calculating analytically the peak force applied to the blade as the product of the velocity at the end of the pipe by the mass flow hitting the blade. Of course some simplification must be assumed like the area of the impacting gas and the distribution of the pressure on the blade airfoil. A similar approach can be followed for oil jets whose higher density is suitable to excite very large blades. Much lower force amplitudes can be reached by speakers which can be calibrated by recording the spectra of a white noise by means of a microphone [12], [13]. The dynamics of the speaker can be recorded and used as a calibration curve in order to guarantee the same intensity at each frequency, while the value can be estimated by measuring the pressure on the microphone multiplied by the area of the speaker. Attention must be paid to the air gap assessment for each blade since a small difference can cause an unacceptable error on the time delay between the harmonic

force profiles which actually load the blades. The force measurement using permanent magnet for rotating disks can be performed by placing a force transducer below the magnet which is fixed to a circular plate. Since the exciter is a single piece, compact device, it can be considered as an additional mass which must be taken into account in order to verify if the frequency upper limit of the force transducer drops to values within the tested bandwidth. In the same way, force transducer can be used with electromagnets as well. Unfortunately, electromagnets are more complex devices than the permanent magnets, since components like conducting wires, packed plates, and insulating materials are assembled together and may generate a non-linear dynamic behaviour of the exciter itself. Similar to piezo-actuators [9], they must be supported by an adequate power amplifier system in order to generate the sufficient force in particular for high frequencies.

In this paper the design, manufacture and calibration of a travelling wave excitation system for bladed disks based on electromagnets are described and tested. The measurements provide accurate results to be compared with numerical prediction.

The essential requisites of a travelling wave excitation system for such kind of tests in presence of inherent mistuning are:

- the absence of contact between blade and exciter
- the same excitation force amplitude on each blade modulated with a given time lag which is determined by the engine order index

If the test setup involves the characterization of non-linearities due to friction the requisites listed above are not enough, since the excitation system should be able to provide:

- high excitation force amplitude in order to produce slipping between the friction contacts,
- accurate measurement of the force amplitude of the rotating force pattern.

The excitation produced by electromagnets (EMs) is non-contact and is then suitable for this kind of measurements. The system hardware and software are purposely designed to satisfy all the requisites listed above. The system set up requires an accurate calibration process aimed at fixing the force exerted on the structure by each EM. The calibration consists of two steps: the first step is based on an instrumented EM which measures the force exerted on the structure, the second step is a tuning process in order to regulate all the other EMs for the generation of the same force amplitude on each blade.

In the first part of the paper the hardware and software of the excitation system setup are described, together with a summary of the theoretical background that is necessary for the EM design. In the second part the system set up and calibration are presented with particular attention on the proposed tuning method that allows the calibration of the EMs on site i.e. under the disk in their final position. In the last part of the paper an example of application on a 24 bladed disk is presented.

The Excitation System Hardware

The excitation system is based on an EM unit (EM + aluminium support) repeated cyclically (as sketched in Fig. 1(a)) in order to excite a cyclic bladed structure (like a bladed disk) with one EM under each blade which is not in contact with the exciter. The force is generated by the magnetic induction flowing through the EM, the air gap and the ferromagnetic material of the blade. The EMs (up to 24) are mounted on an aluminium circular plate [Fig. 1(b)]. The aluminium is chosen in order to not interfere with the magnetic flux flowing in the EMs. Each EM is fed with a voltage with a given amplitude and phase.

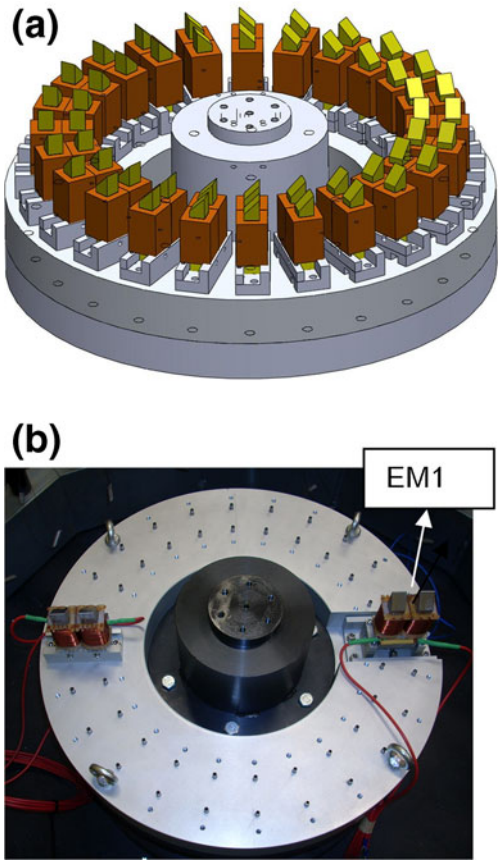

Fig. 1 (**a**) The cyclical excitation system. (**b**) The aluminium circular plate with two EMs

The EM Unit

The EM unit is shown in detail in Fig. 2. Each electromagnet unit is made of two coils (1) of wire wrapped around a U-shaped core of ferromagnetic packed plates.

Two prismatic extensions (2) are glued at the two ends of the U shaped core in order to face the blade at the stagger angle α. This solution was preferred instead of producing single piece EM core in order to change only the prism in case of tests performed on bladed disks with different blade stagger angles. The prismatic extensions are made up of Soft Magnetic Composite (SMC) material which strongly limits eddy currents [17]. The electromagnet is designed in order to satisfy two essential criteria related to 1) the geometry of the structure under test and 2) the maximum force and maximum frequency of the planned travelling wave excitation, in detail:

- the EM size must be limited according to the room between two adjacent blades of the bladed disk under test. In this paper, for instance, the excitation system is designed for a dummy integral bladed disk (blisk) having 24 blades developed. The room between two blades is therefore fixed allowing a maximum square cross area for a commercial EM core $S=16\times16$ mm^2, the U-shaped core outer dimensions are automatically determined: 64×48×16 mm (height × width × thickness).
- The EM must produce a maximum harmonic force amplitude of 15 N in order to excite the structure from 100 Hz to 500 Hz given an air gap l_{air} large enough to consider the variation of the gap during the blade vibration negligible. As a consequence l_{air} is 2 mm minimum and it is considered constant during the design process.

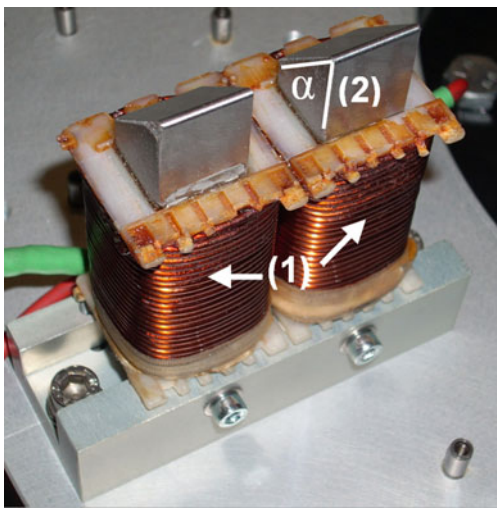

Fig. 2 The Electromagnet (EM) unit

Although the EMs are nominally identical, several issues determine the presence of an error which affects the nominal force generated by different EMs when the same voltage is applied. As it will be demonstrated in the next sections, some issues are related to the manufacture of the EM units itself (windings manufacture, wires length and soldering, prismatic extension gluing, cradle assembly). This kind of errors can be taken into account with a calibration process on a calibration bench. Another kind of issues depends on the EMs assembly under the bladed disk, and in particular they are related to the uncertainties depending on the alignment of the EM units bolted to the aluminium plate which basically produces an error on the actual air gap of each EM facing the blade. For this purpose a tuning process must be performed on site in order to guarantee that all the EMs exert the same force amplitude on the disk. Moreover, the amplitude value of the exciting force must be controlled with accuracy in order to measure the non-linear forced response of the test article at each frequency when the same travelling force is applied within the frequency range of interest (step-sine mode). A special instrumented EM, called Force Measuring ElectroMagnet (FMEM), is designed in order to guarantee the control of the force amplitude.

The Force Measuring Electromagnet (FMEM)

The force measuring electromagnet (FMEM) shown in Fig. 3 substitutes EM1 in the cyclic array [see Fig. 1(b)] during the EMs tuning process. The FMEM includes an EM nominally equal to the other EMs which is mounted on a particular support carrying a piezoelectric force transducer (PCB 208C02). The transducer measures the horizontal component (F_M) generated by the force (F_A) produced by the EM and applied to the blade. The reaction of the vertical component of F_A as well as the mass of the EM is supported by the leaf spring. By knowing the relationship occurring between F_A and F_M, it is possible to control the

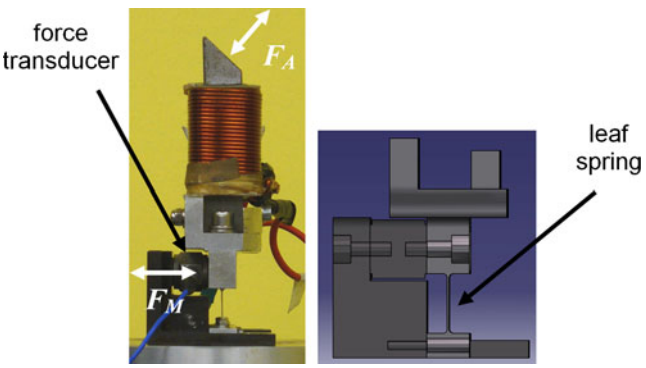

Fig. 3 The force measuring electromagnet (FMEM)

force F_A applied to the blade by controlling the force F_M measured by the force transducer.

Theoretical Background of the Electromagnetic Force

The analytical analysis of the force generated by an electromagnet on a ferromagnetic anchor is described in detail in [14]. Here the main relationships are reminded. The force f generated by an electromagnet with two coils is:

$$f = 2f_{\text{coil}} = 2\left(\frac{B^2 \cdot S'}{2 \cdot \mu_{\text{air}}}\right) \tag{1}$$

where S' is the area of each coil of the EM facing the anchor ($S'=S/\sin(\alpha)$), μ_{air} is the magnetic air permeability, B is the magnetic induction which can be expressed by:

$$B = \frac{N \cdot i \cdot \mu_{\text{air}}}{l_{\text{air}}} \tag{2}$$

where N is the number of turns for each coil, i is the current, l_{air} is the air gap.

When the electromagnet is fed by an alternating current $i(t) = I\sin(\omega t + \varphi)$, with ω electrical angular frequency $\omega = 2\pi f_{el}$ and φ a given phase shift, the force in equation (1) becomes:

$$\begin{aligned} f &= \frac{N^2 \cdot \mu_{\text{air}} \cdot S'}{l_{\text{air}}^2} I^2 sin^2(\omega t + \varphi) = \\ &= \frac{N^2 \cdot \mu_{\text{air}} \cdot S'}{l_{\text{air}}^2} \frac{I^2}{2}(1 - \cos(2\omega t + 2\phi)) = f_s + f_a \end{aligned} \tag{3}$$

where f_s and f_a are the static and the alternate component of the attractive force. In particular the component force f_a

$$\begin{aligned} f_a &= \frac{(N \cdot I)^2 \cdot \mu_{\text{air}} \cdot S'}{2l_{\text{air}}^2} \cos(2\omega t + 2\varphi) \\ &= F_a \cos(2\omega t + 2\varphi) \end{aligned} \tag{4}$$

is the force that excites dynamically the blade. It can be noted from equation (4) that the frequency of f_a is twice the frequency of the applied current i, as well as the phase shift. The blade is then excited with a "mechanical" frequency $f_m = 2\omega/2\pi$ that is two times the "electrical" frequency $f_{el} = \omega/2\pi$. The force amplitude F_A is determined by the product NI. The current amplitude should be limited to a maximum value of 10 A in order to avoid danger for the insulation due to generation of heat. As a consequence if a maximum force amplitude F_A=15 N is required a minimum number of turns N=50 must be provided.

The relationship between the amplitude of the input current I and the amplitude of the input voltage V is given by the admittance quantity $Y=I/V$:

$$Y = \frac{1}{\sqrt{R^2 + \omega^2 L^2}} \tag{5}$$

where L is the inductance of the windings and R the electrical resistance of the conductor wire. It is possible to see that the admittance drops quickly tending asymptotically to zero when the frequency increases. A cut-off frequency is found according to the user needs when a too high voltage amplitude V is required in order to guarantee the current amplitude I, and therefore the force amplitude F_A. The current amplitude I in equation (4) is substituted with the equation (5):

$$\begin{aligned} f_a &= \frac{(NV)^2 \cdot \mu_{\text{air}} \cdot S'}{2 \cdot (R^2 + \omega^2 L^2) \cdot l_{\text{air}}^2} \cos(2\omega t + 2\varphi) \\ &= F_A \cos(2\omega t + 2\varphi) \end{aligned} \tag{6}$$

Equation (6) shows the relationship between the voltage amplitude V, the force amplitude F_A and the input electrical frequency (ω):

$$V^2 = \frac{2 \cdot F_A \cdot (R^2 + \omega^2 L^2) \cdot l_{\text{air}}^2}{\mu_{\text{air}} N^2 \cdot S'} \tag{7}$$

Since $R^2 << \omega^2 L^2$ (R= 0.3 Ω, L= 5.5 mH [14]) equation (7) can be rewritten as:

$$V \approx \sqrt{\frac{2 \cdot F_A \cdot L^2 \cdot l_{\text{air}}^2}{\mu_{\text{air}} N^2 \cdot S'}}\omega \tag{8}$$

As a consequence, if the same value of the force amplitude F_A is constant for the frequency range during step-sine acquisition, the corresponding value of voltage amplitude V feeding the EM changes proportionally with ω. The linear trend V vs. ω of equation (8) will be confirmed by the EMs calibration described in next sections.

The Control Software

The software controls both the excitation system and the vibration measurement which is non-contact since it is performed by a scanning Laser Doppler Vibrometer (LDV). The software module concerning the excitation was purposely implemented in LabVIEW (LV) in order to fulfil the three functions listed below:

1. To perform a force control loop by adjusting the voltage amplitude of the EMs until the measured force signal of a reference force transducer matches a given set-point.

2. To generate simultaneously up to 24 voltage signals by means of a National Instrument CompactRIO platform to supply the EM units with a given amplitude and with the same frequency. The generated signals are shifted in time with a phase lag between each other in order to mimic an *eo*-type rotating force.
3. To provide a trigger function for the scanning LDV Politech in order to measure the Operative Deformed Shape (ODS) of the bladed disk.

Function 1 of the software is used only during the calibration process involving both the FMEM and the EMs, as it will be explained deeply in the next section. The software controls the force measured by the FMEM load cell or the reference load cell on the calibration bench. This control is summarized in the inner loop of Fig. 4. The software controls the force until a set-point force amplitude value is reached, the corresponding voltage value feeding the EM is then stored in order to build up the database of the calibration factors (force vs. voltage).

During the standard step-sine measurement the software works using functions 2 and 3. According to the outer loop of (Fig. 4), for each value of the discretized frequency range, the software generates the 24 harmonic voltages whose amplitude is given by the calibration factors (voltage vs. frequency) stored after EMs calibrations. After a time delay provided by the user to measure the steady response of the bladed disk a trigger signal is sent to the Scanning LDV to start the acquisition. The excitation and measurement are repeated automatically by the software for each frequency of the discretized range.

The software module concerning the laser measurement drives a Politech built-in software which 1) moves the laser beam during scanning, 2) performs the measurement of the velocity for each position and 3) elaborate the Discrete Fourier Transform (DFT) of the velocity signals. Frequency Response Functions (FRFs) are calculated referring the DFT spectrum to the amplitude force at which the calibration factors were measured.

Calibration of the Excitation System

The two main design requirements of the excitation system are:

- each EM should excite its facing blade with the same excitation force amplitude F_A,
- the value of the exciting force generated by the EMs should be known with a good precision.

These requirements are satisfied through different calibration steps that are here summarized and described in detail in the next sections.

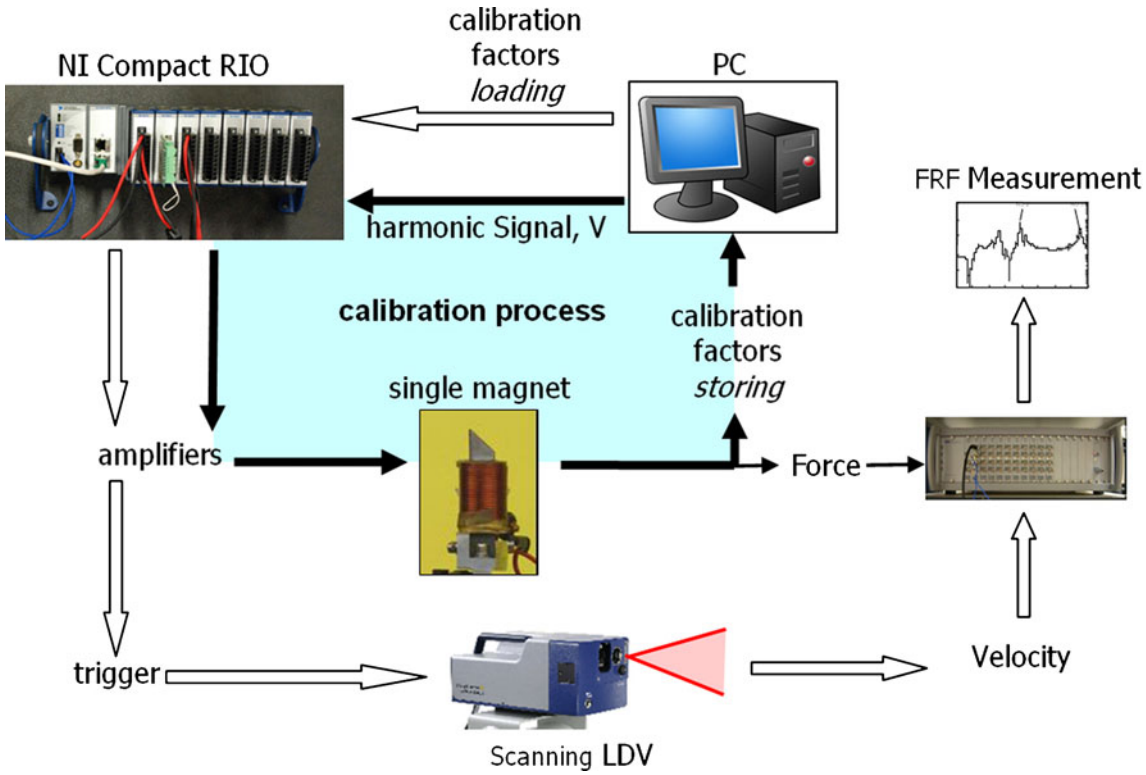

Fig. 4 The excitation and acquisition system

Calibration of the EMS

The 24 EMs are nominally identical, however, in order to check the EMs manufacture quality, each EM is calibrated outside the rig on a purposely designed calibration bench shown in Fig. 5(a). A force transducer (1), carrying a ferromagnetic anchor (2), is connected to an inertial mass (3). The anchor has the same local shape and size of the disk blade that is tested. The part of the inertial mass close to the anchor is made of aluminum (4) in order to not interfere with the magnetic flux. The EM faces the anchor with a given gap (2 mm).

The control software is here used to adjust the harmonic input voltage of the EM amplifier in order to obtain the desired force amplitude (with a tolerance of ±1%) measured by the force transducer connected to the anchor. As expected the force on the anchor is at a frequency that is twice the "electrical frequency" of the applied current signal.

In Fig. 5(b) the calibration curves defined as input voltage amplitude (V) vs. input electrical frequency (f_{el}) are shown for the 24 electromagnets by keeping the force amplitude F_A=5 N constant on the anchor. The repeatability error on the measured voltage values obtained by repositioning the same EM on the rig is 2% maximum. Despite the good calibration repeatability and the nominal equal shape, the calibration curves of the 24 EMs are different from each other. The highest voltage difference for the same electrical frequency is 13% with respect to the mean value . The difference of the calibration curves is associated to the EM manufacture process.

The linear trend of the calibration curves in Fig. 5(b) confirms the validity of the relationship of equation (8) where the amplitude voltage V is proportional to the electrical frequency for a given force amplitude F_A. Furthermore, since the voltage values V corresponding to a force F_A=5 N are known from the calibration process, the generic input voltage values V_{XN} required for a force amplitude F_A=XN≠5 N at a given frequency can be estimated as:

$$V_{XN} = V_{5N}\sqrt{\frac{F_{XN}}{5}}. \tag{9}$$

It must be noted that practically the maximum force amplitude that can be exerted by the EM depends on several factors which can be summarized in:

- air gap
- maximum current amplitude in order to avoid danger for the insulation due to generation of heat, this value depends on the wire material and cross section
- amplifier features: maximum gain, power and input voltage
- electrical admittance (equation (5)) of the EM which depends on the EM resistance and inductance and mainly on the electrical frequency.

Of course, the most limiting feature among the ones listed above determines the performance of the excitation system. For the system here developed, considering the amplifier features, it can be estimated that each EM allows obtaining a maximum of 5 N force amplitude for a mechanical frequency up to 600 Hz and a maximum force amplitude of 15 N for a mechanical frequency up to 300 Hz.

Calibration of the FMEM

The FMEM undergoes a calibration process on the calibration bench before being mounted under the disk [Fig. 6(a)]. The aim is to know the force value F_M that will be controlled by the software corresponding to a given value of the force amplitude F_A on the blade.

The FMEM is constrained to the calibration bench with a gap of 2 mm from the electromagnetic anchor [see Fig. 6(a)] and is fed by a harmonic voltage in a given range of electrical frequency. The control software adjusts the harmonic input voltage of the FMEM amplifier in order to obtain the desired force amplitude F_A (with a tolerance of ±1%) on the transducer supporting the anchor at a frequency that is twice f_{el}. At the same time the force amplitude F_M is measured by the FMEM transducer and recorded.

The ratio F_M/F_A is plotted vs. the electrical frequency f_{el} in Fig. 6(b) showing that the FMEM has a natural frequency in the range of the chosen electrical frequencies. A hammer test has confirmed the presence of a resonance of the FMEM at a mechanical frequency of 206 Hz (which corresponds to an electrical frequency f_{el}=103 Hz). The system showed a linear dynamic behaviour only far from

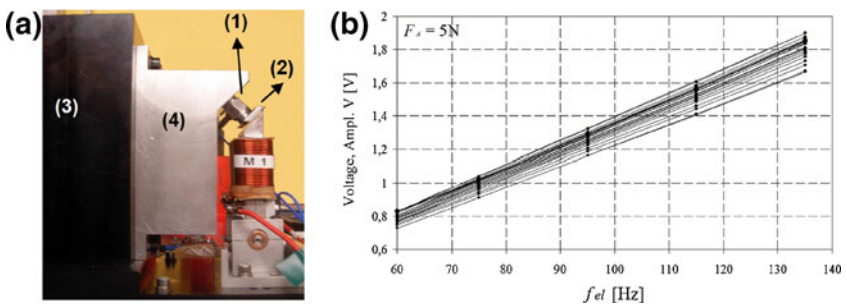

Fig. 5 (**a**) The EM on the calibration bench. (**b**) The 24 EMs calibration curves

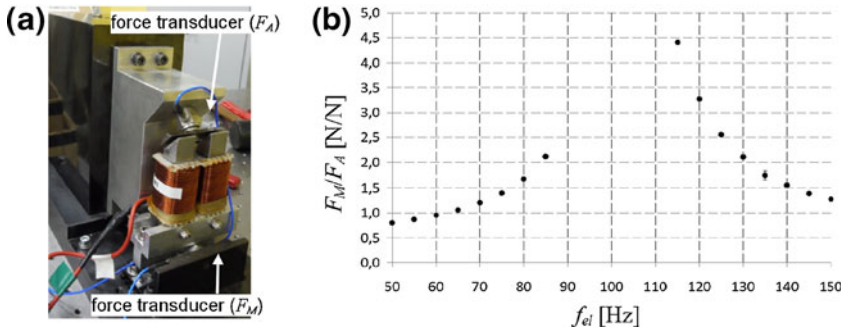

Fig. 6 (**a**) The FMEM on the calibration bench, (**b**) Calibration curve of the FMEM

the natural frequency since the transfer function F_M/F_A does not change by varying the excitation force F_A. In order to avoid the poor measurement repeatability due to non-linearities, the FMEM is employed only in the ranges of frequency outside the resonant condition (f_{el}=50→85 Hz and f_{el}=130→150 Hz). The calibration curve F_M/F_A plotted in Fig. 6(b) is the average result of three curves obtained after repositioning the FMEM on the calibration bench and after gap adjustment to 2 mm. This calibration curve will be called $(F_M/F_A)_{AVG}$.

After this first calibration an "inverse calibration" is performed on the same bench in order to simulate the same control force procedure that will be adopted on site under the bladed disk. In this case the FMEM transducer that measures F_M is controlled by the software. The set-point controlled by the software at different frequencies is F_M= $(F_M/F_A)_{AVG}$·$F_{A,nom}$ where $F_{A,nom}$= 5 N is the nominal force value. When the FMEM transducer reaches the target value of force F_M, the actual force $F_{A,act}$ exerted on the anchor is measured. The average error of $F_{A,act}$ with respect to the nominal force value of 5 N is 2.8% in the electrical frequency range 50→85 Hz and 2.6% in the electrical frequency range 130→150 Hz. It can then be concluded that the control of F_M by means of the FMEM transducer through the calibration curve $(F_M/F_A)_{AVG}$ of Fig. 6(b) leads to an actual force on the anchor that is $F_{A,nom}$ with an error lower than 3%. Further tests are performed by changing the gap (2.5 mm instead of 2 mm) and keeping as calibration curve $(F_M/F_A)_{AVG}$ to verify if the calibration curve can be still used. In this cases the measured value of the force $F_{A,act}$ on the anchor shows differences from 5 N not higher than 5%.

The Method for Tuning the EMS

The EMs tuning involves a voltage regulations "on site" under the bladed disk. An example of integral bladed disk (blisk) having N_b=24 blades is shown in Fig. 7(a). The tuning on site requires the measurements of the vibration response of the blades. This measurement is performed by means of the scanning LDV which detects the blade velocity along the disk axial direction. One measurement point is chosen for each blade in the same position.

Two system configurations are needed for this calibration:

- configuration 1: only the FMEM is needed under blade 1;
- configuration 2: the 24 EM units are positioned under the bladed disk (after removal of the FMEM).

In the configuration 1 the FMEM is switched on (the other 23 EMs can be positioned under the disk but inoperative). The FMEM is fed with an alternate voltage at an electrical frequency f_{el}. The mechanical excitation frequency value (that is two times f_{el}) is chosen as far as

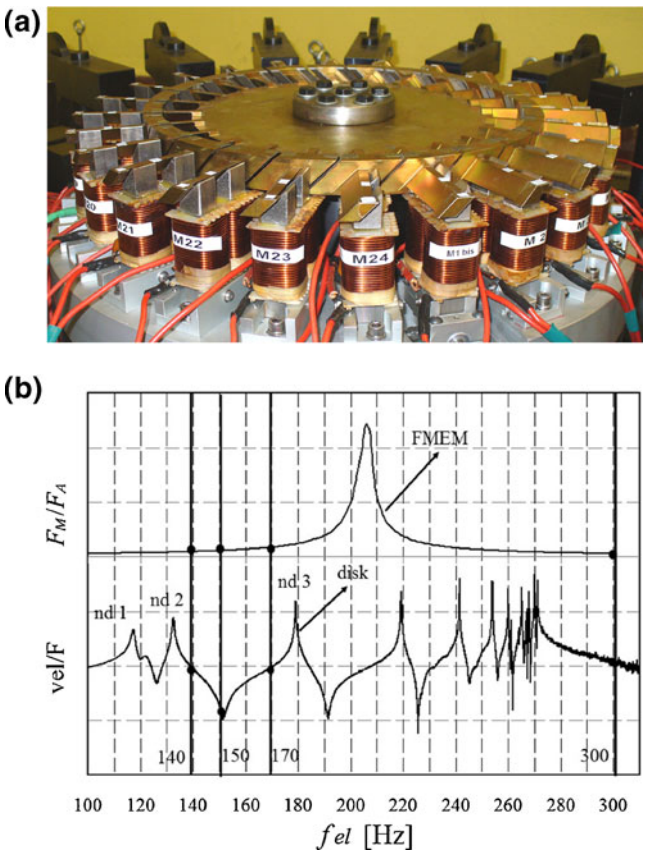

Fig. 7 (**a**) The 24 EMs under the bladed disk. (**b**) transfer function for the FMEM and FRF for the bladed disk (y-axis is not to scale)

possible from the disk and from the FMEM resonances in order to avoid calibration complications due to disk or FMEM dynamics. The disk FRF and the FMEM transfer function measured by impact testing are shown in Fig. 7(b). Each resonance of the bladed disk is characterized by a circumferential modal shape having a number of nodal lines (nodal diameters nd) where the modal displacements are zero. The labels nd=1, 2, and 3 in the figure indicate the disk peak resonances for couple of modal shapes. The two modes of each pair have the following features: 1) they vibrate at resonance for the same natural frequency value, 2) they have the same number of nd and 3) they are orthogonal, i.e., the scalar product of the two mode shapes is null. The four mechanical excitation frequencies f_m chosen for the tuning process (140, 150, 170, 300 Hz) are also highlighted in the same figure. In particular, the highest chosen frequency value (300 Hz) which is far from the bladed disk resonances allows covering the whole first family dynamics of the blisk characterized by the first out-of-plane bending mode of the blade whose last resonant frequency in the figure is around 270 Hz. In order to excite the bladed disk with the excitation frequencies of the tuning process, the FMEM must be supplied with an input voltage with half value electrical frequency (f_{el}=70, 75, 85, 150 Hz).

At a given f_{el} the control software regulates the voltage amplitude feeding the FMEM with a control loop on the FMEM force transducer [see Fig. 6(a)] in order to reach the target value F_M which corresponds to $F_{A,nom}$ on blade 1. The set-point value $F_M=(F_M/F_A)_{AVG}\ F_{A,nom}$ was previously obtained from the calibration curve of Fig. 6(b) for different f_{el} values. Once the force control loop has reached the target value at $f_m=2f_{el}$, a trigger signal activates the scanning LDV to measure the velocity amplitude of the 24 blades. The blade velocity amplitudes vs. the blade number (velocity profile) are plotted in Fig. 8(a) and (b) for the four values of f_{el} feeding the FMEM.

The velocity profiles of Fig. 8(a) and (b) are kept as reference profiles for the tuning process since they are obtained with a known force amplitude of 5 N (measured on site) on the excited blade.

The system is then set up in configuration 2: the FMEM is removed, the 24 EMs are positioned under the disk as shown in Fig. 7(a). Only one EM per time is switched on. Figure 9(a) shows the 24 velocity amplitude profiles at the excitation electrical frequency f_{el}=75 Hz when the calibration curves of Fig. 5(b) are used as initial voltage amplitude for the 24 EMs. Each velocity profile is measured when one EM per time excites the structure. The velocity amplitude of the directly excited blade is plotted always in the first position (Blade Order 1). On the same figure the velocity reference profile (bold line) obtained with the FMEM at f_{el}=75 Hz in the previous

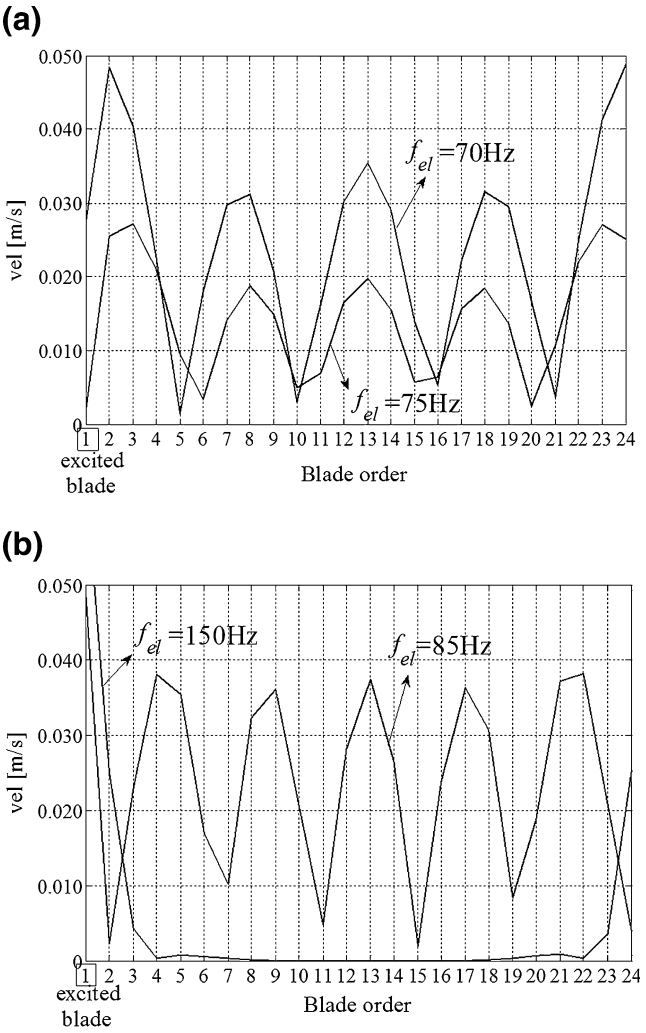

Fig. 8 Velocity amplitude profile when the FMEM is switched on, force controlled to a nominal force amplitude $F_{A,nom}$=5 N: (**a**) electrical frequency 70 Hz and 75 Hz, (**b**) electrical frequency 85 Hz and 150 Hz

step (configuration 1) is plotted. The curves of Fig. 9(a) point out two phenomena:

- there are relevant differences among the velocity profiles when the working EM exciter changes (the standard deviation of the force values compared to the mean value of the force is about 16%),
- the velocity profile obtained by FMEM is higher than the others.

Assuming the dynamics of the blisk linear and neglecting the presence of mistuning phenomena since the excitation frequency is far from resonance conditions, the differences among the profiles in Fig. 9(a) must be referred to different excitation force amplitudes. These differences are not related to the manufacture of the EM units since they are taken into account in the calibration curves of Fig. 5(b). Other causes producing different velocity profiles

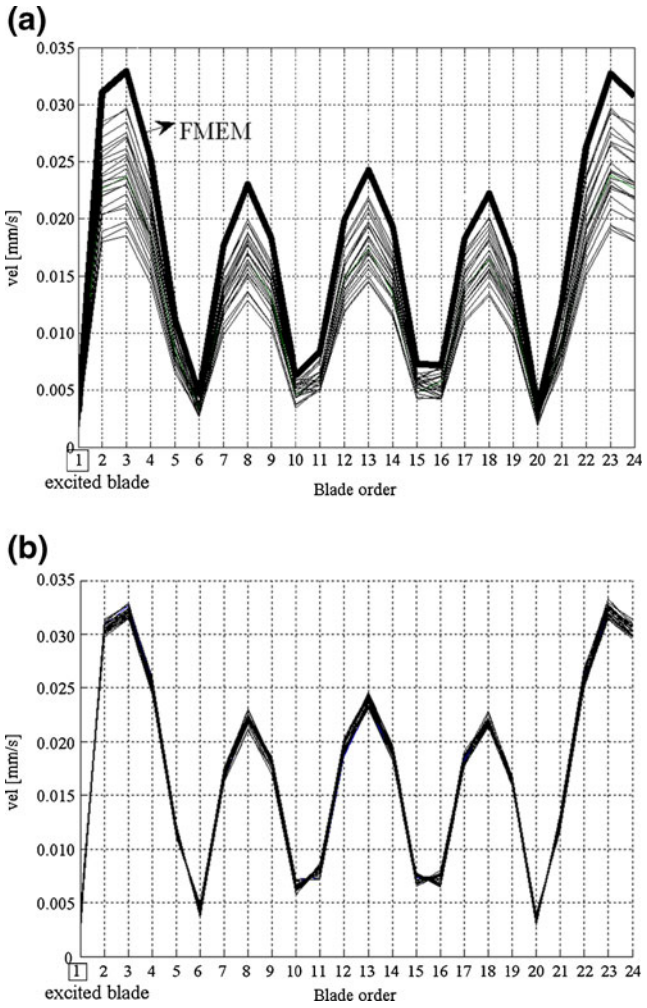

Fig. 9 The 24 velocity profiles, each of them measured with one EM switched on, at f_{el}=75 Hz and nominal force amplitude $F_{A,nom}$=5 N: (**a**) before tuning, (**b**) after tuning

are probably due to 1) different positions of the EMs under the disk blades that cause different air gaps, 2) different shape and material properties of the blade compared to the anchor used for calibration since the average velocity profile of the 24 EMs is 25% lower than the reference profile (FMEM). The velocity profile obtained by FMEM under the bladed disk is higher than those obtained with EMs simply calibrated on the bench since the actual voltage required to excite the blades at the same value of F_A is higher than the voltages measured on the calibration bench. This is probably due to the higher magnetic field loss in the blade connected to the disk compared to the case of the single magnetic anchor on the calibration bench. This evidence highlights the importance of having a FMEM measuring the real force amplitude exerted by the EM on site (i.e. under the disk) since the calibration on the bench outside the disk revealed to be not enough.

The tuning process aims at adjusting the voltage on the 24 EMs until they produce the same velocity profiles of the blisk as the one measured with the FMEM working. A method is here proposed starting from the velocity profiles shown in Fig. 9(a). The voltages are adjusted in order to obtain 24 velocity profiles overlapping the FMEM reference profile as shown in Fig. 9(b).

In detail the method works as follows. Let $\dot{X}_{be}$ and $\dot{X}_{bFMEM}$ be the measured velocity amplitudes of the blade corresponding to the blade order b when respectively the EM e and the FMEM is switched on. Considering the system linear and assuming the FMEM as reference, the ratio $\dot{X}_{be}/\dot{X}_{bFMEM}$ is proportional to the excitation force ratio $F_{A,e}/F_{A,\mathrm{FMEM}}$ where $F_{A,e}$ is the actual excitation force amplitude on the blade facing the EM e and $F_{A,FMEM}$ is the nominal value of the force (in this case 5 N). For each response of Fig. 9(a) (corresponding to the e-th EM working) the correction factor k_e is calculated as:

$$k_e = mean\left(\frac{\dot{X}_{be}}{\dot{X}_{bFMEM}}\right), \quad b = 1, ..., N_b \tag{10}$$

In order to get the same force amplitude for each EM unit the force is corrected as $F_{A,e}{}^*=F_{A,e}/k_e$ by adjusting the input voltage as $V_e^* = V_e/\sqrt{k_e}$ since the voltage is proportional to the square root of the force (equation (9)). The velocity profiles plotted in Fig. 9(b) are measured after two iterations of the tuning process at f_{el}=75 Hz. The dispersion of the force amplitude corresponding to the different velocity profiles with respect to the nominal value of 5 N are less than 2%. It can be concluded that after this tuning process each of the 24 EMs produces on the excited blade the same force amplitude of 5 N with a dispersion of 2%. The same calibration procedure is repeated for the other electrical frequency values (fel=70, 85, 150 Hz) in order to characterize the linear trend of the voltage as a function of frequency when the same force $F_M=(F_M/F_A)_{AVG}\cdot F_{A,nom}$ is required, as it was done in the calibration bench [Fig. 5(b)] but in this case the results are obtained with the EMs under the disk. The linear trend of equation (8) is confirmed hence the voltage values at frequencies not directly tuned can be found by linear interpolation.

It must be noted that the tuning method here proposed is very efficient since it avoids the calibration of one EM at a time on a separate bench which is time consuming. In fact, the tuning process does not require a particular starting voltage value of the EMs, in particular it is not necessary to start with voltage values coming from the EMs calibration [Fig. 5(b)].

Application of the Excitation System to a Bladed Disk

The developed excitation system is applied to generate a rotating force pattern on the dummy blisk shown in Fig. 7(a). The entire experimental set up is shown in Fig. 10(a). The disk above the EM excitation system is in the

foreground. The amplifiers, the control system and the PC are in the back. Figure 10(b) shows the response measurement system with the laser pointing to a complete reflective mirror fixed on the roof. The beam is redirected to the tip of the blades in order to collect the circumferential Operative Deflection Shape (ODS) of the blisk. The sample test here presented consists of the excitation of the blisk in its linear configuration, i.e. without sources of intentional nonlinearity (underplatform dampers or shrouds).

The force amplitude is limited to F_A=0.1 N since the blisk is characterized by a really low structural damping and will be excited at resonance condition. A force pattern is provided in order to generate an *eo* type travelling excitation:

$$f_n = F_A \cos(\omega_m t + (n-1)\varphi_m), \quad n = 1, ..., N_b \tag{11}$$

with $\omega_m = 2\pi f_m$. The quantity $\varphi_m = (2\pi/N_b)\cdot eo$ is called Inter Blade Phase Angle (IBPA) and determines the time lag of the harmonic excitation of one blade with respect to the contiguous ones. It must be reminded that the electrical signals feedind the EMs in terms of frequency and phase shift must be the half of the corresponding mechanical values according to equation (6):

$$\omega_m = 2\omega = 2(2\pi f_{el}) \rightarrow f_{el} = \frac{\omega_m}{4\pi} \qquad \phi_m = 2\varphi \rightarrow \varphi = \frac{\varphi_m}{2} \tag{12}$$

Measurements are performed in two excitation conditions around the resonance peaks of respectively *nd*=2 and *nd*=3 [see Fig. 7(b)]:

1. F_A=0.1 N, *eo*=2 that is IBPA=$\pi/6$ for a frequency range 125–140 Hz (f_{el}=63–70 Hz);
2. F_A=0.1 N, *eo*=3 that is IBPA=$\pi/4$ frequency range 170–185 Hz (f_{el}=85–92.5 Hz).

the correct voltage values to feed the EMs at a given frequency are obtained by linear interpolation from the calibrated voltages.

The laser measured responses of the disk in the two excitation conditions are shown in the 3D plot of Fig. 11(a) and (b). Each 3D plot includes the FRFs of the 24 blades. Both plots show that the FRF are not the same for each blade as can be expected in the case of an ideal perfect bladed disk excited by an *eo* type excitation with the same force amplitude on each blade. In both cases the FRF amplitudes are modulated by a spatial wave along the circumferential coordinate composed of different vibration amplitudes of each blade. In case 1 [Fig. 11(a)] the spatial wave has 4 lobes while in case 2 [Fig. 11(b)] 6 lobes are present. These modulated responses are typical of a bladed disk with a small mistuning (that is with small differences between sectors). The effect of small mistuning is a small splitting of the resonant frequencies of two orthogonal twin modes which are a characteristic of the dynamics of tuned rotors. The two orthogonal modes, which are related to the same nodal diameter, vibrate in resonance condition at two different frequency values instead of the same frequency value as in the tuned case.

The generation of the lobes due to small mistuned rotating ODS is explained qualitatively with an example in Fig. 12. In Fig. 12(a) the FRF of one blade is sketched. The vibration amplitude at a frequency f_m close to the split twin modes is mainly the result of a linear combination (with different modal participation factors) of the two orthogonal modal shapes called mode 1 and mode 2 in Fig. 12(b) and (c). In this example a vibration of the disk close to the *nd*=2 twin modes is assumed. In the same figure the linear combination of the two modal shapes for different time instants is called sum [Fig. 12(d)]. It is possible to see that the resulting rotating ODS changes the amplitude during rotation. The global effect after one rotation [Fig. 12(e)] is a modulation of the rotating *nd*=2 ODS vibration amplitude characterized by 4 fixed lobes. For the same reason Fig. 11(a) shows 4 lobes corresponding to a mistuned rotating ODS at *nd*=2, while 6 lobes are visible in Fig. 11(b) since a mistuned rotating ODS at *nd*=3 is generated.

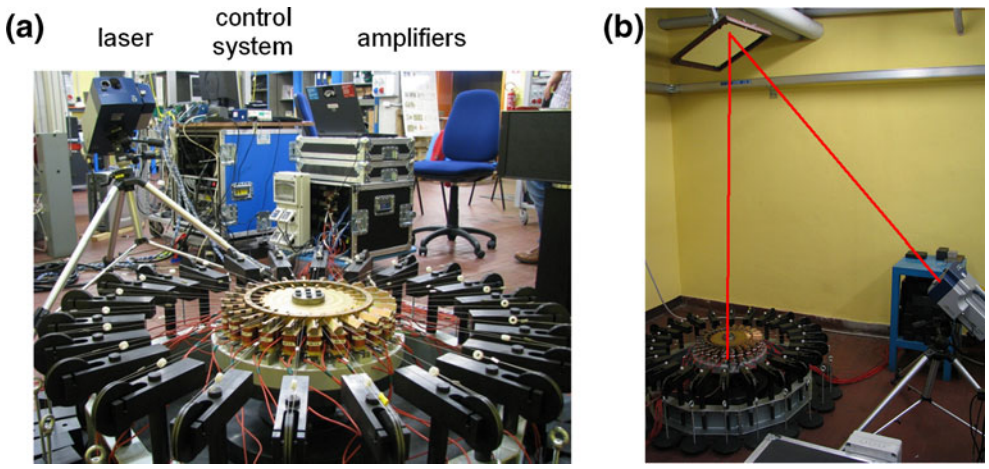

Fig. 10 Experimental set-up

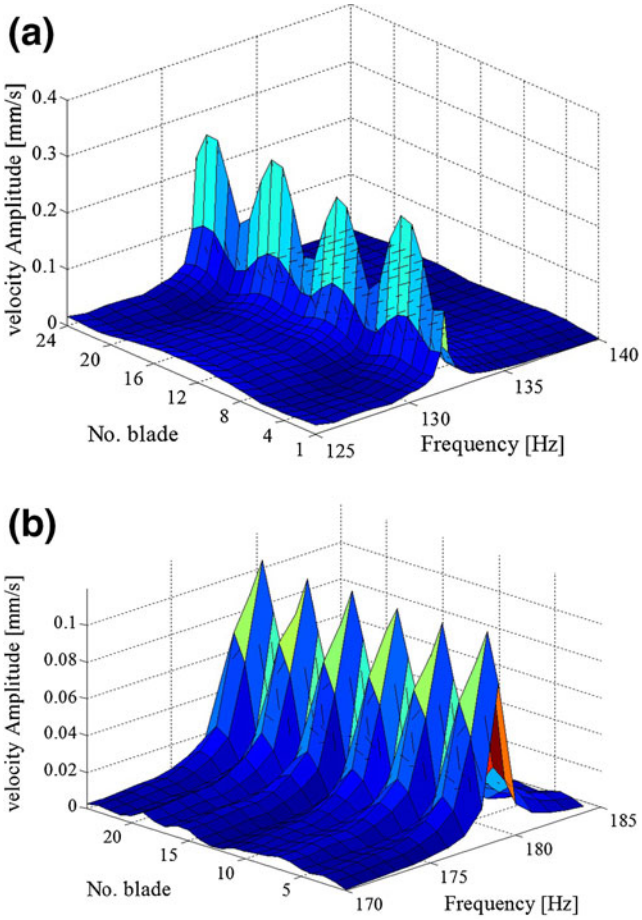

Fig. 11 24 mistuned FRFs of the blisk around the (**a**) nd=2 and (**b**) nd=3 travelling mode

The measurements of Fig. 11 show the presence of small mistuning that is not visible in the results of the hammer test of Fig. 7(b) since there is not apparently peak splitting in the peaks at *nd*=2 and *nd*=3. It is important to notice that the present noncontact excitation system together with laser measurement response allows to appreciate these phenomena related to small inherent mistuning that are not detectable by conventional techniques of mistuning identification based on the frequency split detection. The frequency split is actually a very small percentage of its former values (less than 1%) therefore it is not always possible to experimentally distinguish two separated peaks.

Conclusions

In this paper the design, calibration procedure and testing of a complete (hardware and software) non-contact excitation system is presented. The system aims at performing accurate measurements of the dynamic behaviour of bladed disks in presence of mistuning and non linearity due to friction contacts. The system yields accurate results and it is characterized by three key features.

First, the purposely designed EMs generate force amplitudes that can be considered high for a non contact excitation system. Each EM can reach a force amplitude up to 15 N for a mechanical excitation frequency up to 300 Hz and 5 N for a mechanical excitation frequency up to 600 Hz. In the paper the several features affecting this force value are highlighted.

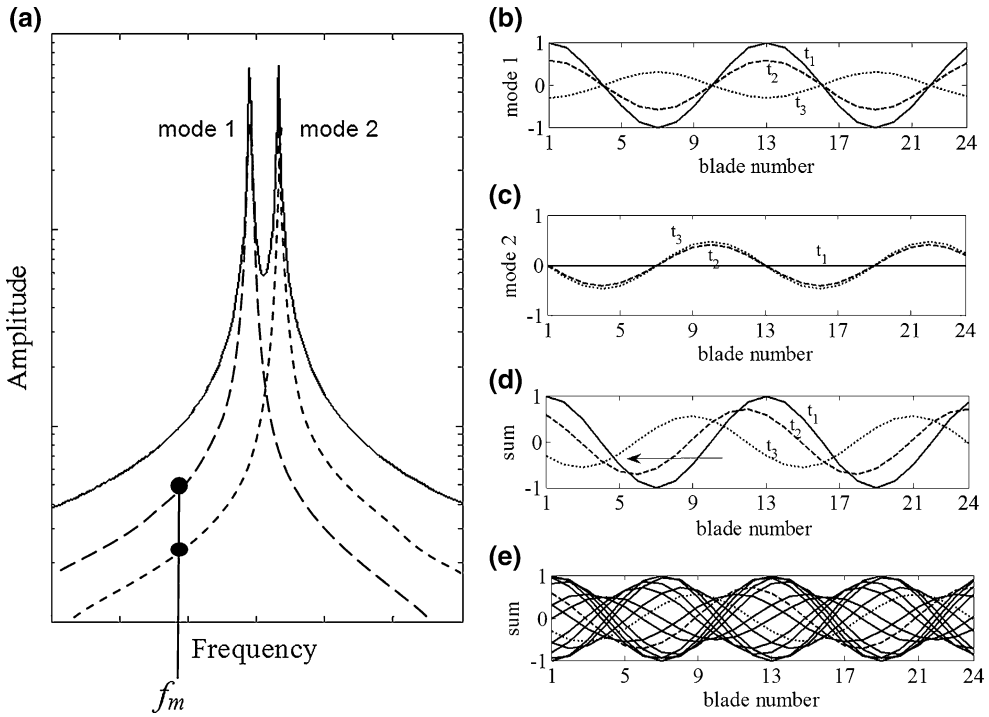

Fig. 12 Example of frequency splitting (**a**) and mistuned modal shape (nd=2) combination: mode 1 deflection shape (**b**), mode 2 deflection shape (**c**), summation of mode 1 and mode 2 (**d**), final result after one complete rotation (**e**)

Second, thanks to a novel calibration method performed on site under the disk to iteratively calibrate the force, differences of force amplitudes among the blades are highly reduced (2% variation among force amplitudes). The method is efficient since it avoids the calibration of each EM (one by one) which is time consuming and in any case it proved to be inaccurate when the EMs are mounted under the blisk.

Third the value of the force amplitude exciting the blades is known with good accuracy (less than 5% error with respect to the nominal value). This feature is essential for stepped sine, force controlled tests to investigate the nonlinearity due to friction contacts. A device carrying one of the EMs and instrumented with a force transducer is designed, constructed and calibrated for this purpose. The device called FMEM (force measurement electromagnet) is able to measure the force directly on site under the disk and is used as a reference for the other EMs during calibration.

The travelling excitation system is applied to excite an integral bladed disk with a given *eo*-type rotating force in order to measure the FRF using step-sine mode around two resonant peaks. The test campaign provided preliminary results which reveal that the system is capable of engine order type excitation at a given force amplitude. Moreover the developed travelling excitation system together with a laser measurement response system allows to highlight the presence of inherent small mistuning not detectable by means of other more conventional techniques.

References

1. Castanier MP, Pierre C (2006) Modeling and analysis of mistuned bladed disk vibration: status and emerging directions. J Propuls Power 22(2):384–396. doi:10.2514/1.16345, ISSN 0748–4658
2. Thomas DL (1979) Dynamics of rotationally periodic structures. Int J Numer Methods Eng 14:81–102
3. Kenyon JA, Griffin JH (2003) Experimental demonstration of maximum mistuned bladed disk forced response. J Turbomach 125(4):673–681. doi:10.1115/1.1624847
4. Pierre C, Judge J, Ceccio SL, Castanier MP (2002) Experimental Investigation of the effects of random and intentional mistuning on the vibration of bladed disks. Proc. of the 7th National High Cycle Fatigue Conference, Palm Beach, Florida
5. Petrov E, Hennings H, Di Mare L, Elliott R (2010) Forced response of mistuned bladed discs in gas flow: a comparative study of predictions and full-scale experimental results. J Eng Gas Turbines Power 132(5):052504. doi:10.1115/1.3205031, ISSN: 0742–4795
6. Avalos J, Mignolet MP (2008) On damping entire bladed disks through dampers on only a few blades, paper code GT-2008-51446. Proc. of ASME Turbo Expo, June 9–13, Berlin, Germany
7. Gotting F, Sextro W, Panning L, Popp K (2004) Systematic mistuning of bladed disk assemblies with friction contacts, paper code GT2004-53310. Proc. of ASME Turbo Expo, June 14–17, Vienna, Austria
8. Beirov B, Kühhorn A, Schrape S (2008) A discrete model to consider the influence of the air flow on blade vibrations of an intergral blisk compressor rotor, paper code GT2008-50613. Proc. of ASME Turbo Expo, June 9–13, Berlin, Germany
9. Kruse MJ, Pierre C (1997) An experimental investigation of vibration localization in bladed disks, part II: forced response. Proc. of the 42nd ASME Gas Turbine & Aeroengine Congress, User's Symposium & Exposition, Orlando, Florida
10. Strehlau U, Kuhhorn A (2010) Experimental and numerical investigations of HPC blisks with a focus on travelling waves, paper code GT2010-22463. Proc. of ASME Turbo Expo, June 14–18, Glasgow, UK
11. Kruse MJ, Pierre C (1997) An experimental investigation of vibration localization in bladed disks, part I: free response. Proc. of the 42nd ASME Gas Turbine & Aeroengine Congress, User's Symposium & Exposition, Orlando, Florida
12. Judge J, Ceccio SL, Pierre C (2003) Traveling-wave excitation and optical measurement techniques for non-contact investigation of bladed disk dynamics. Shock vibr dig 35(3):183–910, ISSN 1741–3184
13. Jones KW, Cross CJ (2003) Travelling wave excitation system for bladed disks. J Propul Power 19:135–141, ISSN 0748–4658
14. Berruti T, Firrone CM, Gola MM (2010) A test rig for non-contact travelling wave excitation of a bladed disk with underplatform dampers, paper code GT2010-22879. ASME Turbo Expo 2010:1–9
15. Chang JY, Wickert JA (2002) Measurement and analysis of modulated doublet mode response in mock bladed disks. J Sound Vib 250(3):379–400. doi:10.1006/jsvi.2001.3942
16. Szwedowicz J, Secall-Wimmel T, Dünck-Kerst P, Sonnenschein A, Regnery D, Westfahl M (2007) Scaling concept for axial turbine stages with loosely assembled friction bolts: the linear dynamic assessment, part I, paper code GT2007-27502. Proc. of ASME Turbo Expo, May 14–17, Montreal, Canada
17. Shokrollahi H, Janghorban K (2007) Soft magnetic composite materials (SMCs). J Mater Process Technol 189(1–3):1–12, 10.1016/j.jmatprotec.2007.02.034